Supporting Information:

Tetrahex Carbides: Two-Dimensional Group-IV Materials for Nanoelectronics and Photocatalytic Water Splitting

Mehmet Emin Kilic* and Kwang-Ryeol Lee*

Computational Science Center, Korea Institute of Science and Technology, Seoul 136-791, Republic of Korea

E-mail: mekilic@kist.re.kr; krlee@kist.re.kr

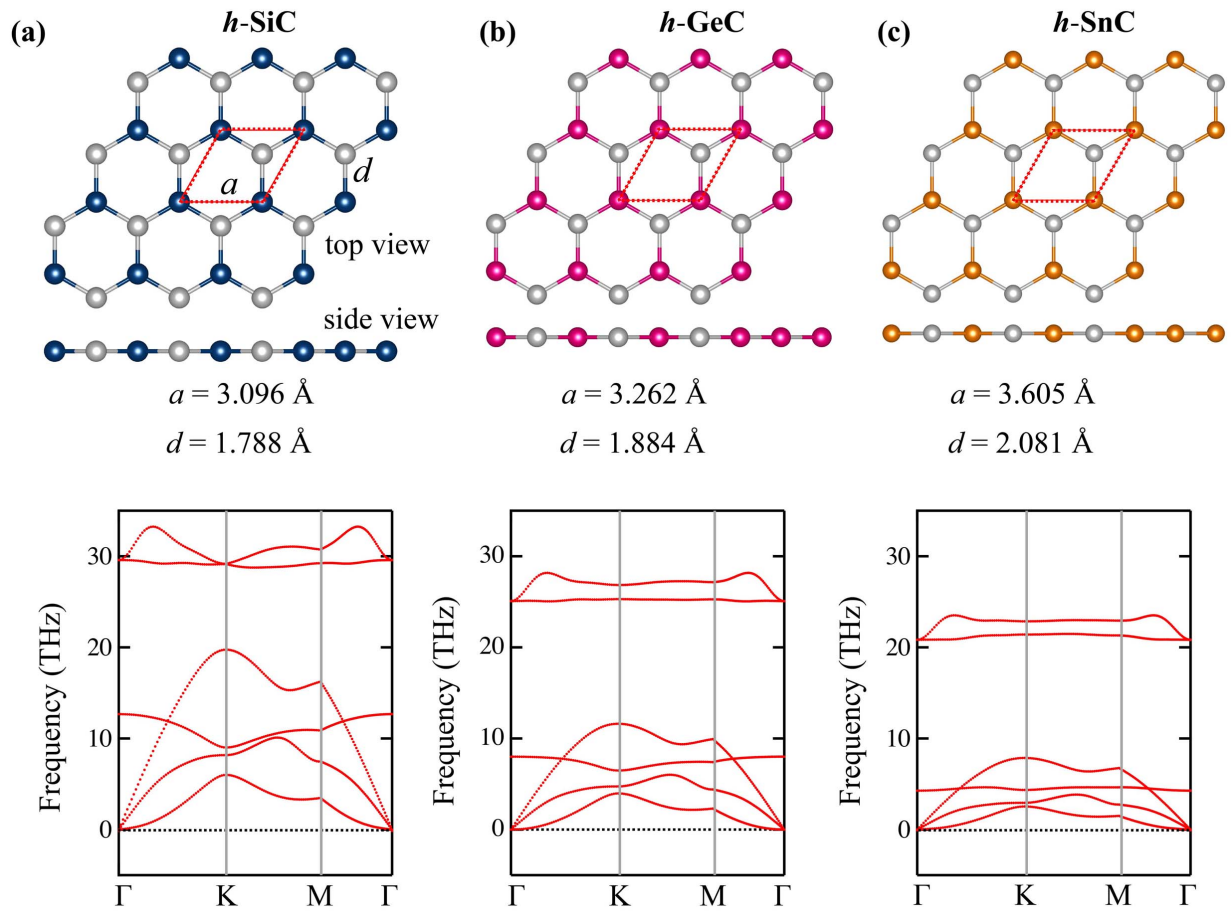

Figure S1: Upper panel: Top and side views of atomic configurations of graphene-like group-IV binary carbides (h-XC (X = Si, Ge, Sn)). (a) h-SiC, (b) h-GeC, and (c) h-SnC, containing one X and one C atoms in the unit cell (framed by the red dashed line). Lattice constants of a and bond length of d are depicted. Blue, pink, orange, and gray spheres in the lattice represent Si, Ge, Sn, and C atoms, respectively. Lower panel: Phonon dispersion curve along with the high symmetric k points in the Brillouin zone. The results indicate that the h-XC compounds have totally positive phonon modes, indicating their dynamics stability. The optimized lattice parameters of h-XC compounds agree well with those obtained by Sahin *et. al*[1]

References

(1) Şahin, H.; Cahangirov, S.; Topsakal, M.; Bekaroglu, E.; Akturk, E.; Senger, R. T.; Ciraci, S. Monolayer Honeycomb Structures of Group-IV Elements and III-V binary Compounds: First-Principles Calculations. *Phys. Rev. B* **2009**, *80*, 155453.

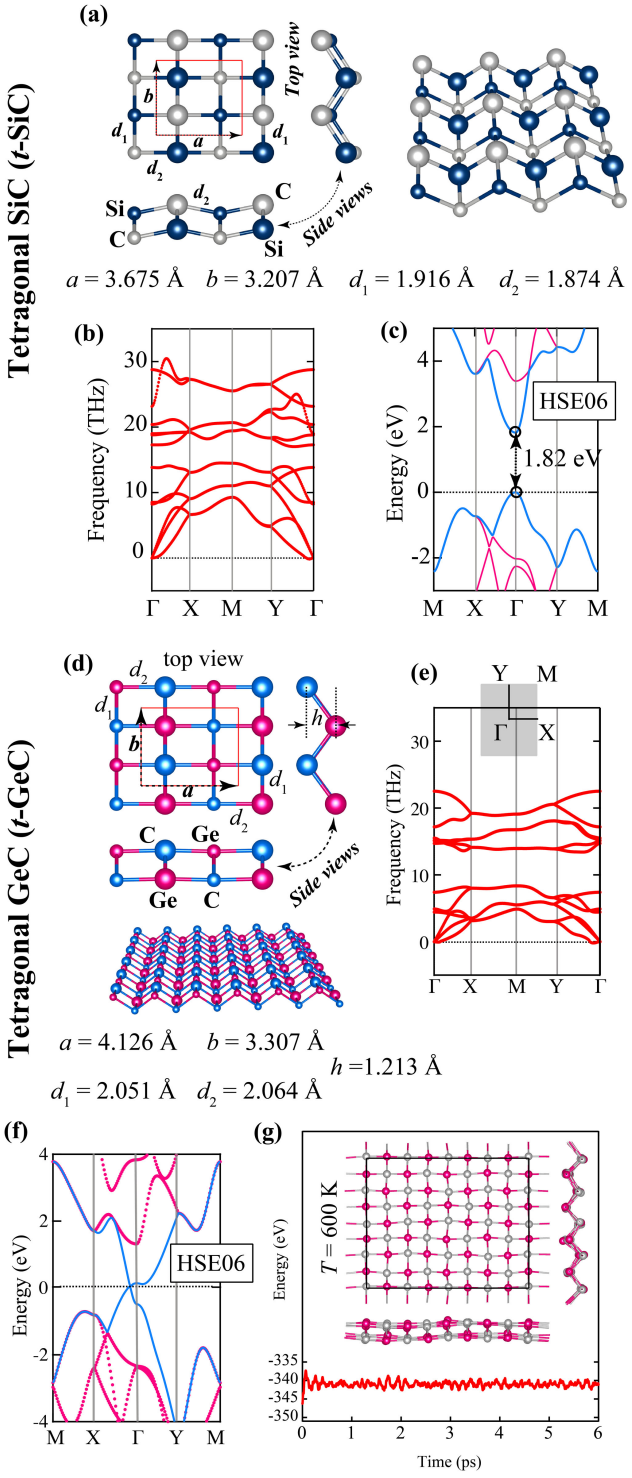

Figure S2: Top view and side views of atomic configurations of (a) tetragonal silicon carbide (t-SiC) and (d) germanium carbide (t-GeC), containing two Si/Ge and two C atoms in the unit cell (framed by the red line). Phonon dispersion curve of (b) t-SiC and (e) t-GeC along with the high symmetric k points in the Brillouin zone. The results indicate that t-SiC and t-GeC have totally positive phonon modes, indicating their dynamics stability. Electronic band structures obtained from the HSE06 functional method for (c) t-SiC and (f) t-GeC. (g) Variation of total potential energy of t-GeC during the AIMD simulations at 600 K for 6 ps.

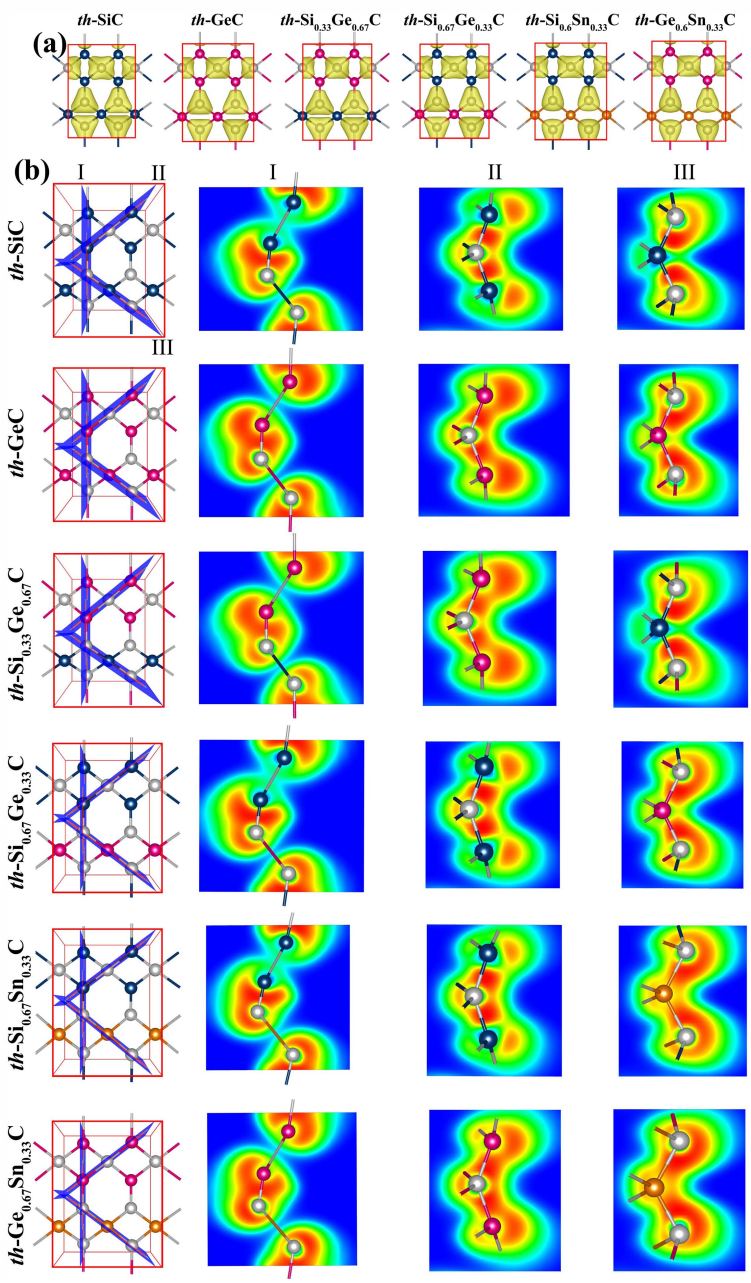

Figure S3: (a) Total charge density of *th*-XC compounds (X = Si, Ge, $Si_{0.33}Ge_{0.67}$, $Si_{0.67}Ge_{0.33}$, $Si_{0.67}Sn_{0.33}$, and $Ge_{0.67}Sn_{0.33}$). The charge density iso-surface (yellow color lobes) is 0.08 e/Å^3. (b) Electron local function (ELF) of *th*-XC compounds. The specific 2D-slice projections are chosen to show the bonds between 3-fold coordinated X and C atoms (X^3-C^3) as depicted plane I, between 3-fold coordinated X and 4-fold coordinated carbon atoms (X^3-C^4) as depicted plane II, and between 4-fold coordinated X and 3-fold coordinated carbon atoms (X^4-C^3) as depicted plane III, where X is Si, Ge, or Sn. Here, gray, blue, pink, and orange spheres represent C, Si, Ge, and Sn atoms, respectively.

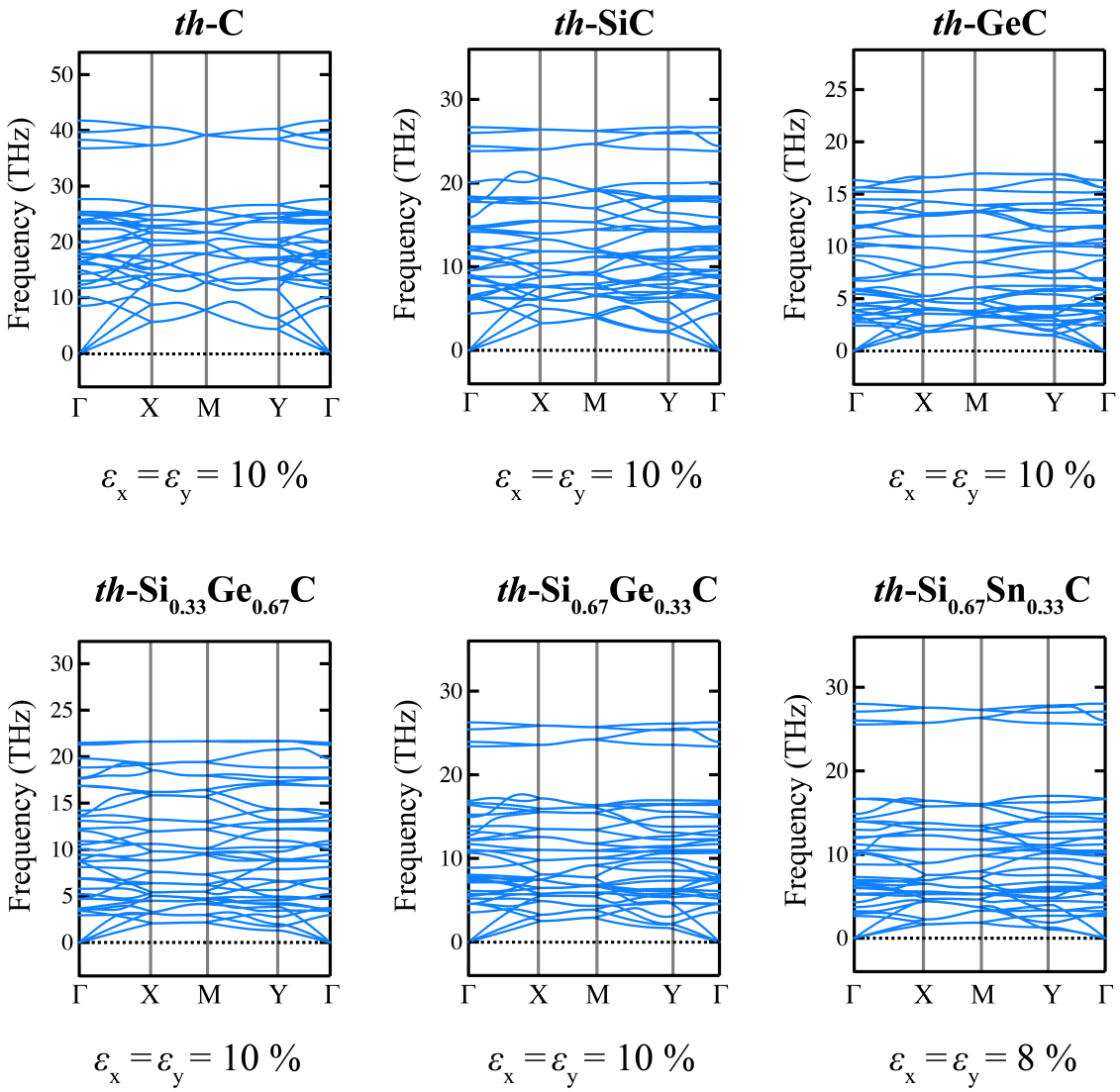

Figure S4: Phonon dispersion curves of *th*-C and *th*-XC compounds where X is Si, Ge, $Si_{0.33}Ge_{0.67}$, $Si_{0.67}Ge_{0.33}$, $Si_{0.67}Sn_{0.33}$ when subjected to ∼10% equi-biaxial tensile strain. It is noted that *th*-$Ge_{0.67}Sn_{0.33}C$ structure shows imaginary phonon modes after 5% equi-biaxial tensile strain.

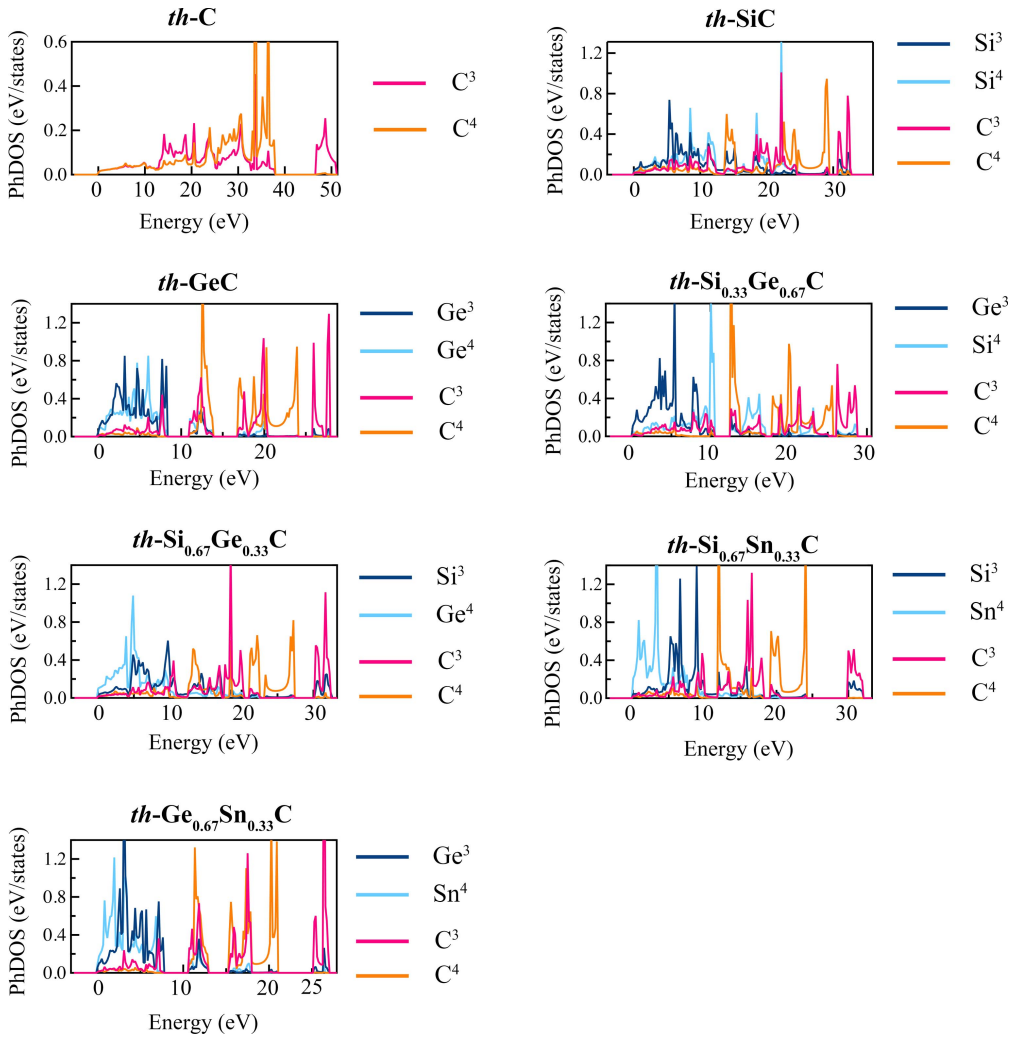

Figure S5: Atom-resolved phonon density of states (PhDOS) of *th*-C and *th*-XC compounds (X = Si, Ge, $Si_{0.33}Ge_{0.67}$, $Si_{0.67}Ge_{0.33}$, $Si_{0.67}Sn_{0.33}$, and $Ge_{0.67}Sn_{0.33}$). The PhDOS of 3- and 4-fold coordinated X atoms (X^3 and X^4) and carbon atoms (C^3 and C^4) are depicted in dark blue, sky blue, pink, and orange colors, respectively.

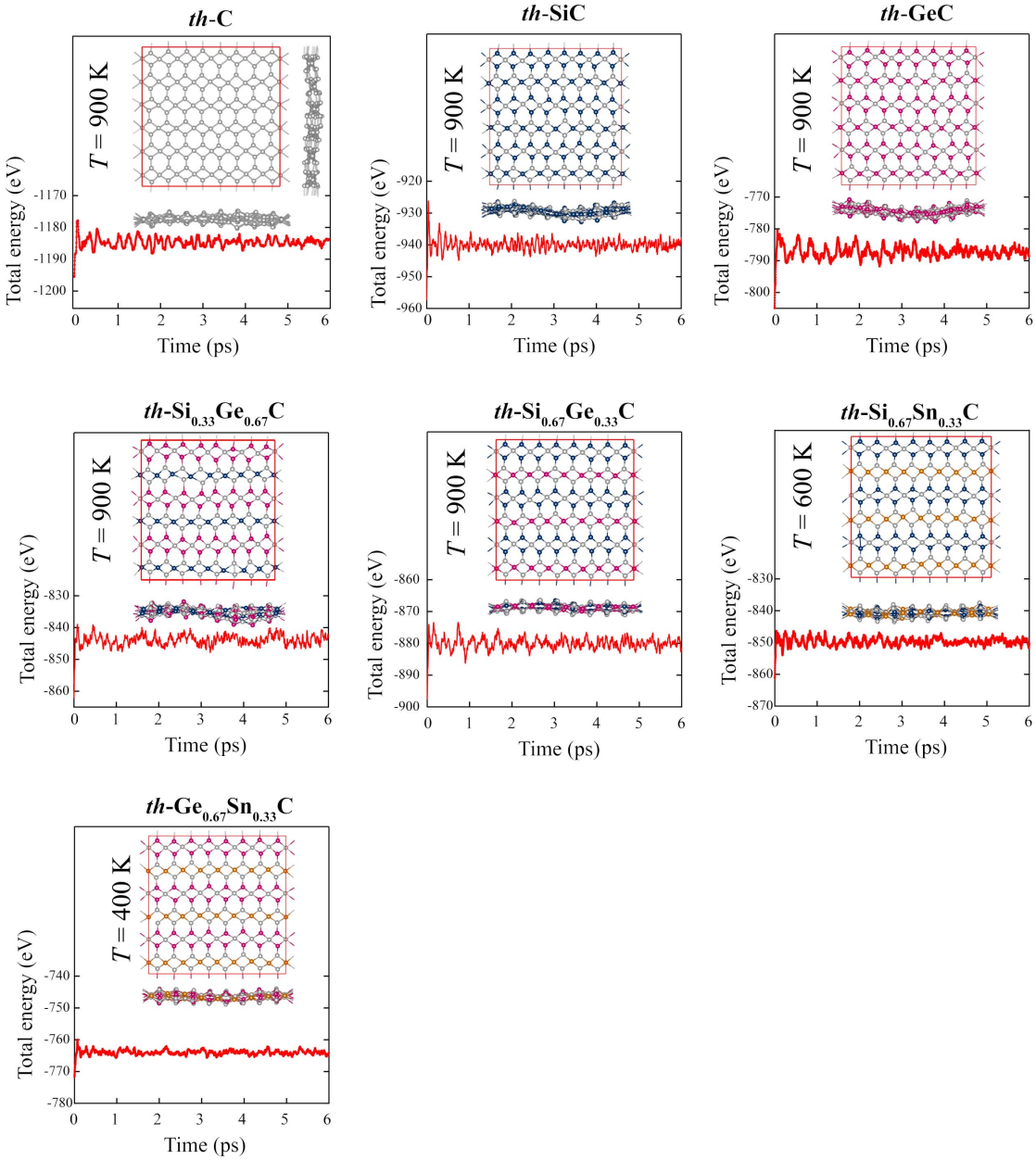

Figure S6: Variation of total potential energy of *th*-C and *th*-XC compounds (X = Si, Ge, $Si_{0.33}Ge_{0.67}$, $Si_{0.67}Ge_{0.33}$, $Si_{0.67}Sn_{0.33}$, and $Ge_{0.67}Sn_{0.33}$) during the AIMD simulations under given temperatures. The insets are snapshots of the atomic structures at the end of simulations. The gray, blue, pink, and orange balls represent C, Si, Ge, and Sn atoms, respectively.

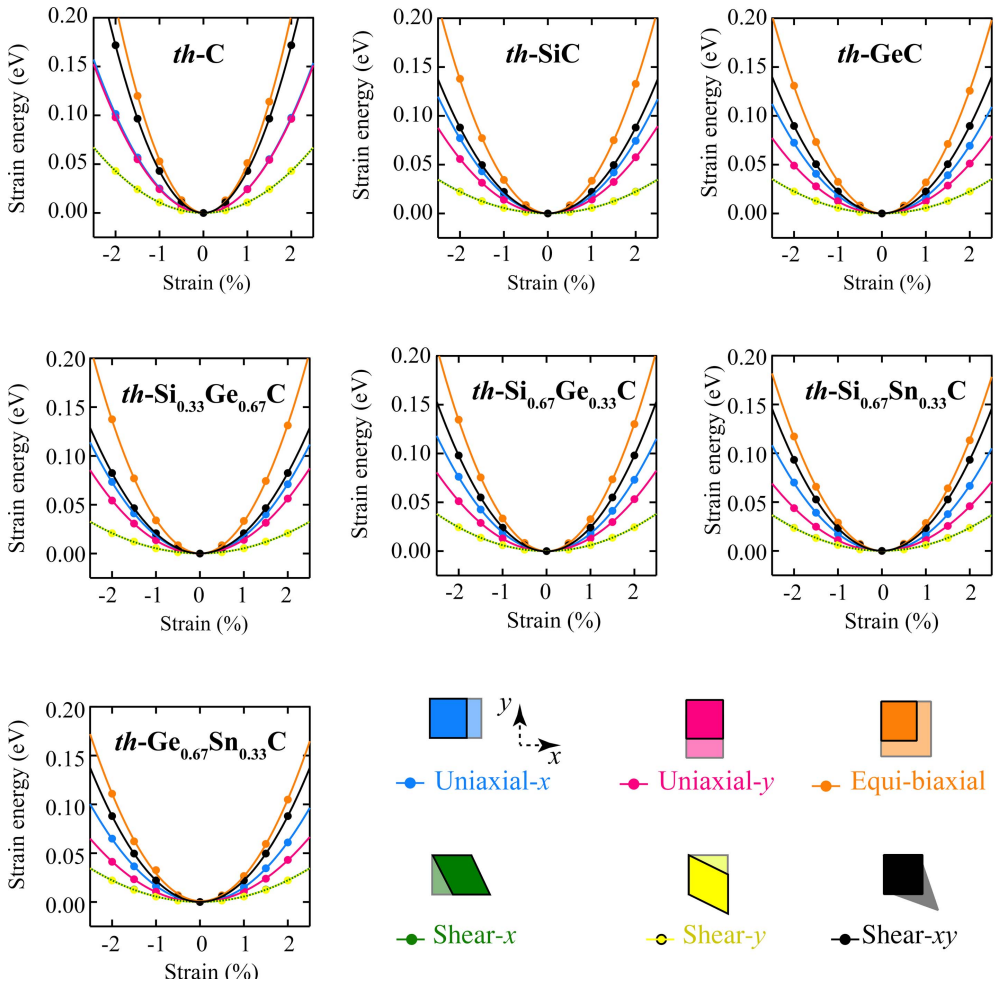

Figure S7: Calculated strain energy of *th*-C and *th*-XC compounds (X = Si, Ge, $Si_{0.33}Ge_{0.67}$, $Si_{0.67}Ge_{0.33}$, $Si_{0.67}Sn_{0.33}$, and $Ge_{0.67}Sn_{0.33}$) with respect to various applied strains: uniaxial strain along the x- and y-directions, equi-biaxial strain, and shear strains.

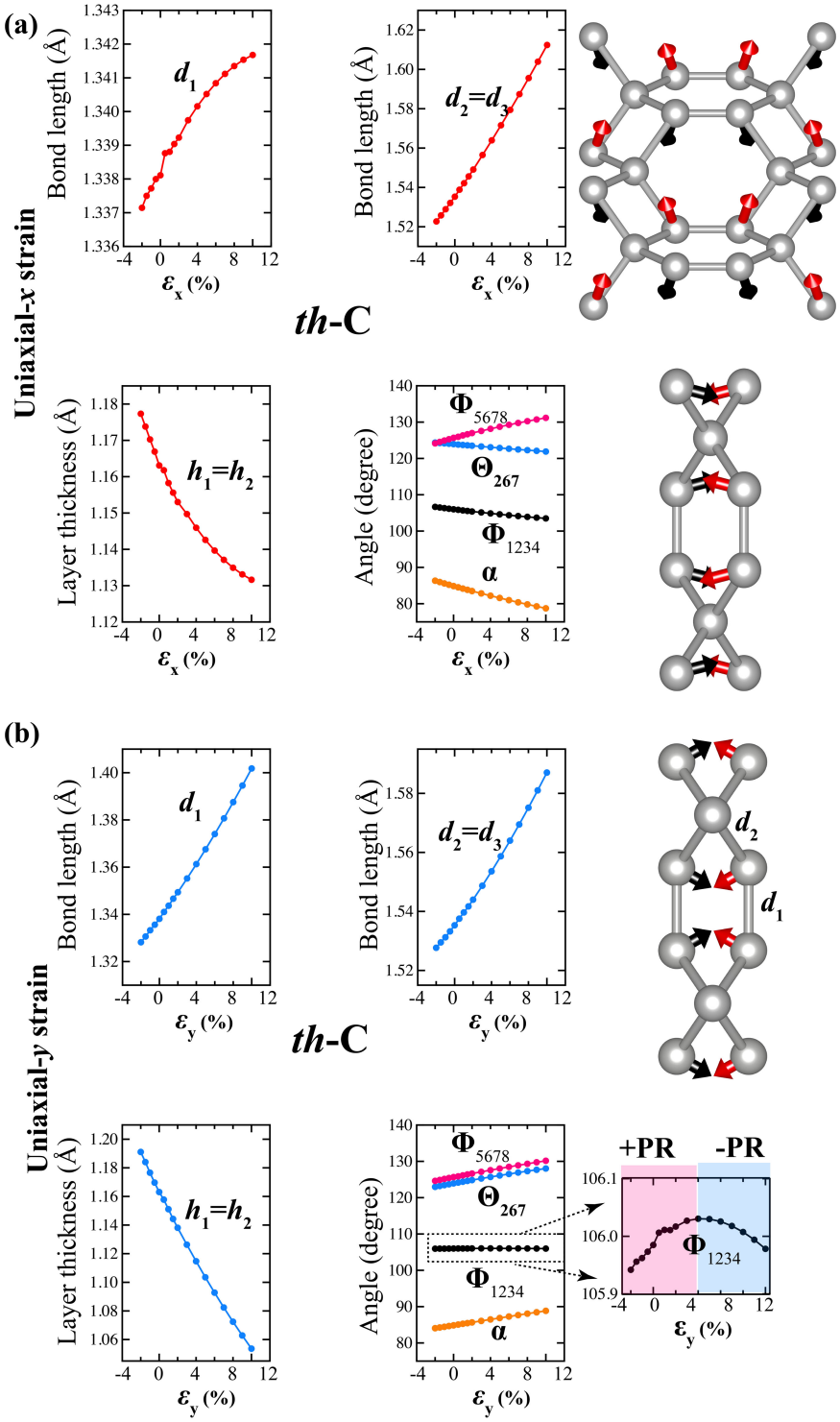

Figure S8: The variation of bond length d_1, d_2, and d_3, buckling height h_1 and h_2, bond angles, and dihedral angles for *th*-C with respect to uniaxial-x strain (ε_x) and uniaxial-y strain (ε_y). Black and red arrows point out the moving direction of carbon atoms when the *th*-C is subjected to uniaxial-x and uniaxial-y strains.

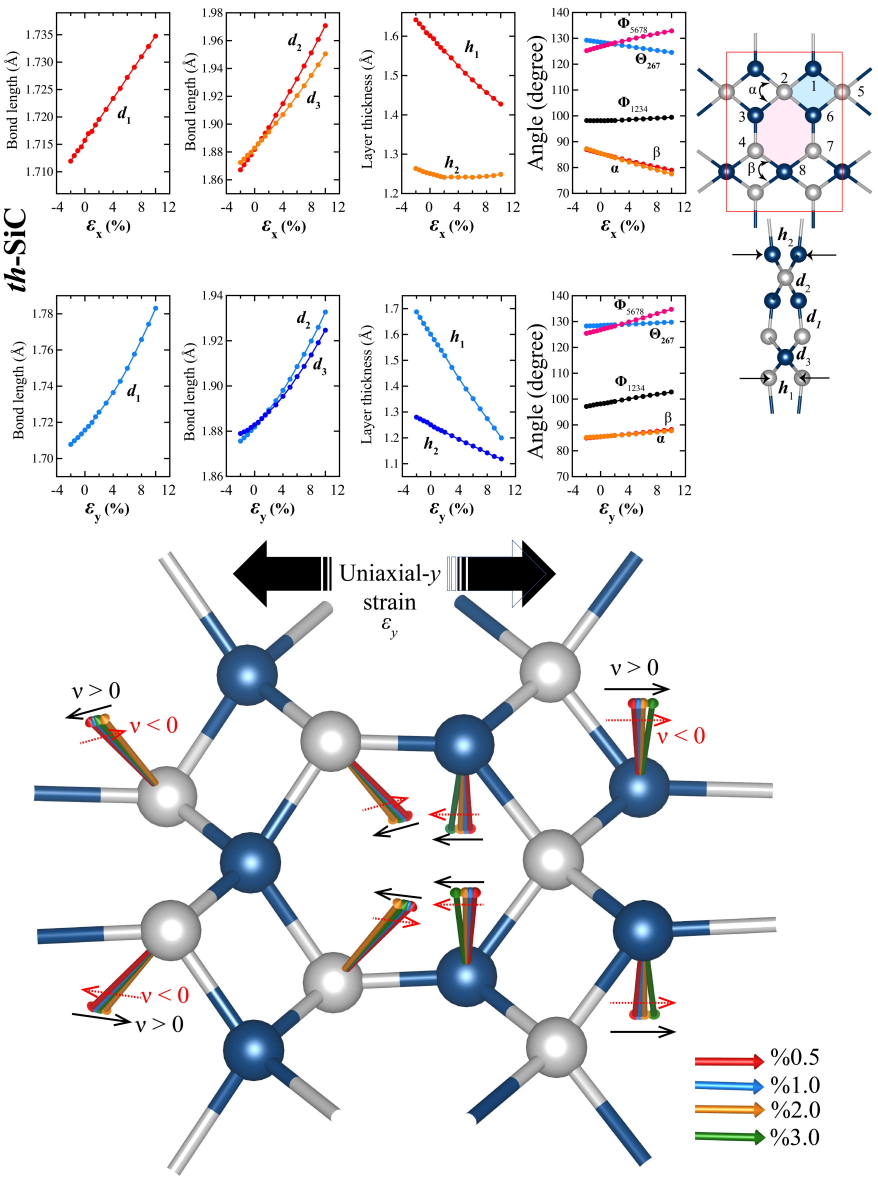

Figure S9: The variation of bond length d_1, d_2, and d_3, buckling height of h_1 and h_2, bond angles, and dihedral angles for *th*-SiC with respect to (a) uniaxial-x strain (ε_x) and (b) uniaxial-y strain (ε_y). The variation of the moving direction of the X and C atoms with respect to the applied uniaxial-y strain is depicted in lower panel.

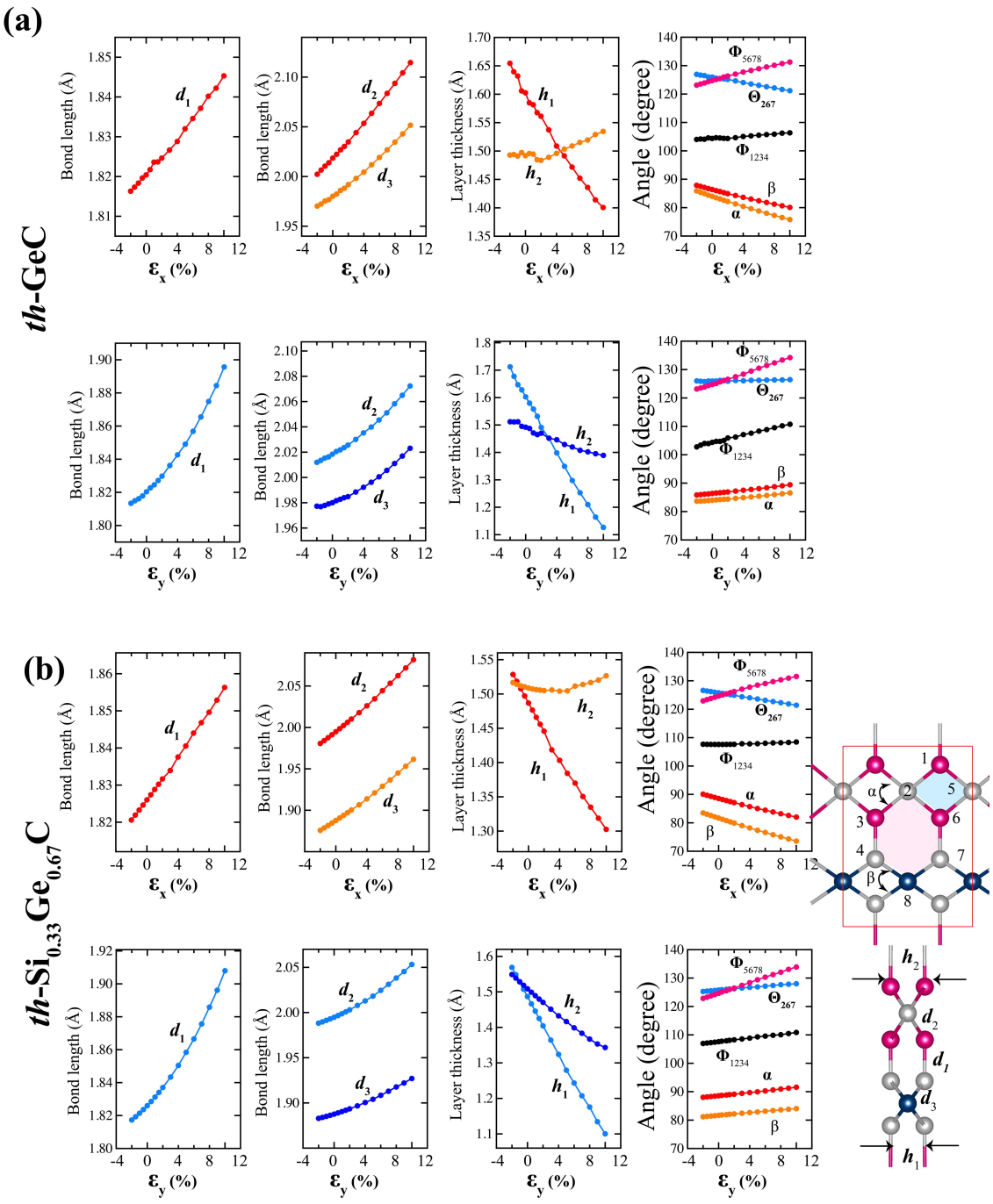

Figure S10: The variation of bond length d_1, d_2, and d_3, buckling height h_1 and h_2, bond angles, and dihedral angles for *th*-GeC and $Si_{0.33}Ge_{0.67}C$ with respect to uniaxial-x strain (ε_x) and uniaxial-y strain (ε_y).

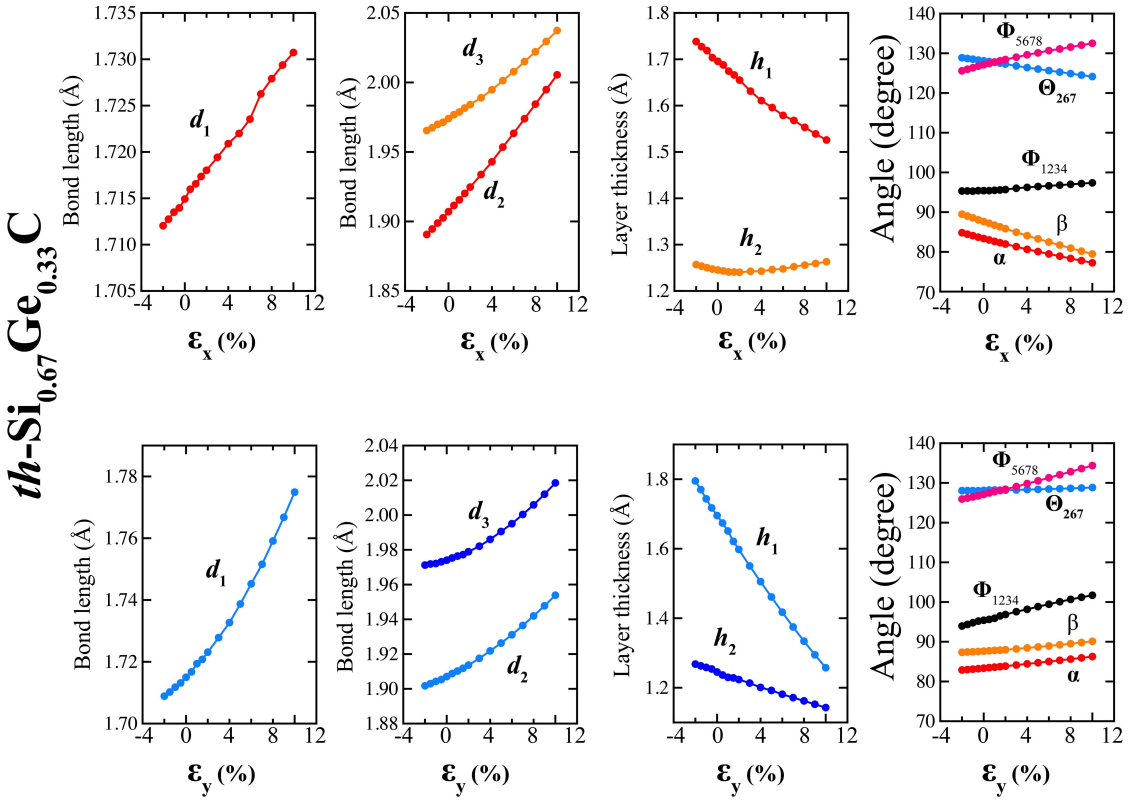

Figure S11: The variation of bond length d_1, d_2, and d_3, buckling height h_1 and h_2, bond angles, and dihedral angles for th-$Si_{0.67}Ge_{0.33}C$ with respect to uniaxial-x strain (ε_x) and uniaxial-y strain (ε_y).

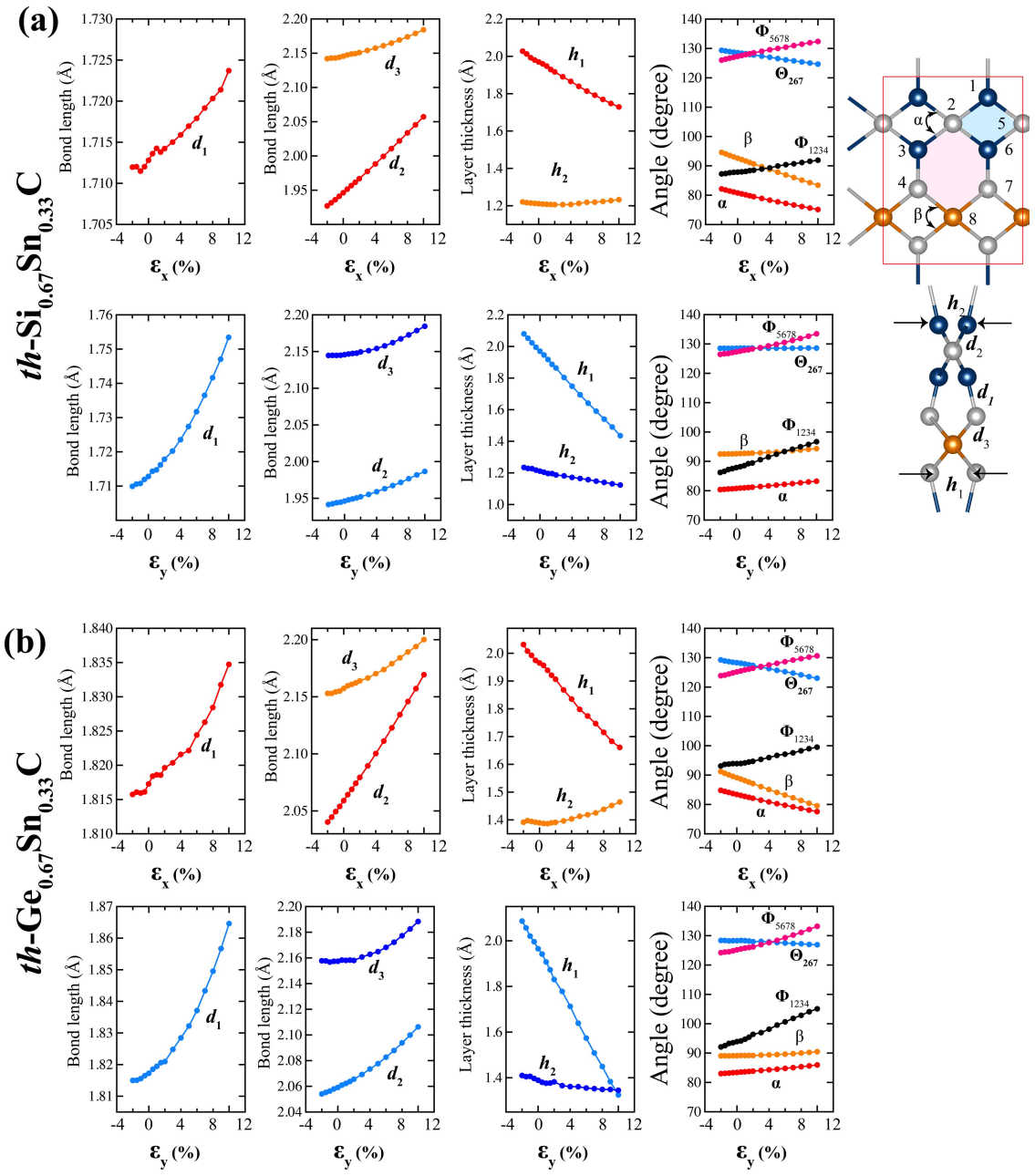

Figure S12: The variation of bond length of d_1, d_2, and d_3, buckling height of h_1 and h_2, bond angles, and dihedral angles for *th*-$Si_{0.67}Sn_{0.33}C$ and *th*-$Ge_{0.67}Sn_{0.33}C$ with respect to uniaxial-x strain (ε_x) and uniaxial-y strain (ε_y).

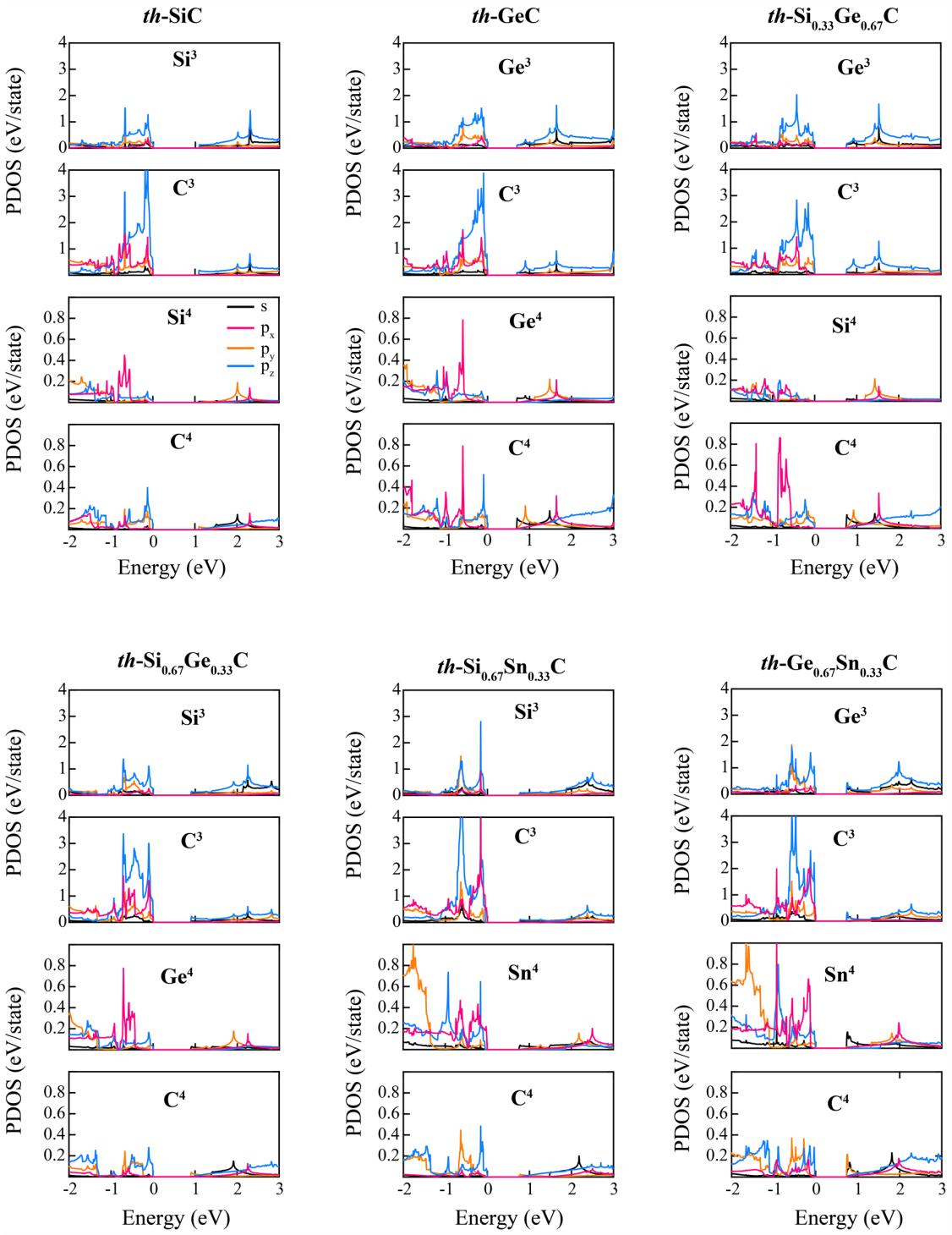

Figure S13: Electronic density of states (DOS) of *th*-XC compounds (X = Si, Ge, $Si_{0.33}Ge_{0.67}$, $Si_{0.67}Ge_{0.33}$, $Si_{0.67}Sn_{0.33}$, and $Ge_{0.67}Sn_{0.33}$). Here, black, pink, orange, sky blue represent s, p_x, p_y, and p_z orbitals of *th*-XC compounds, respectively.

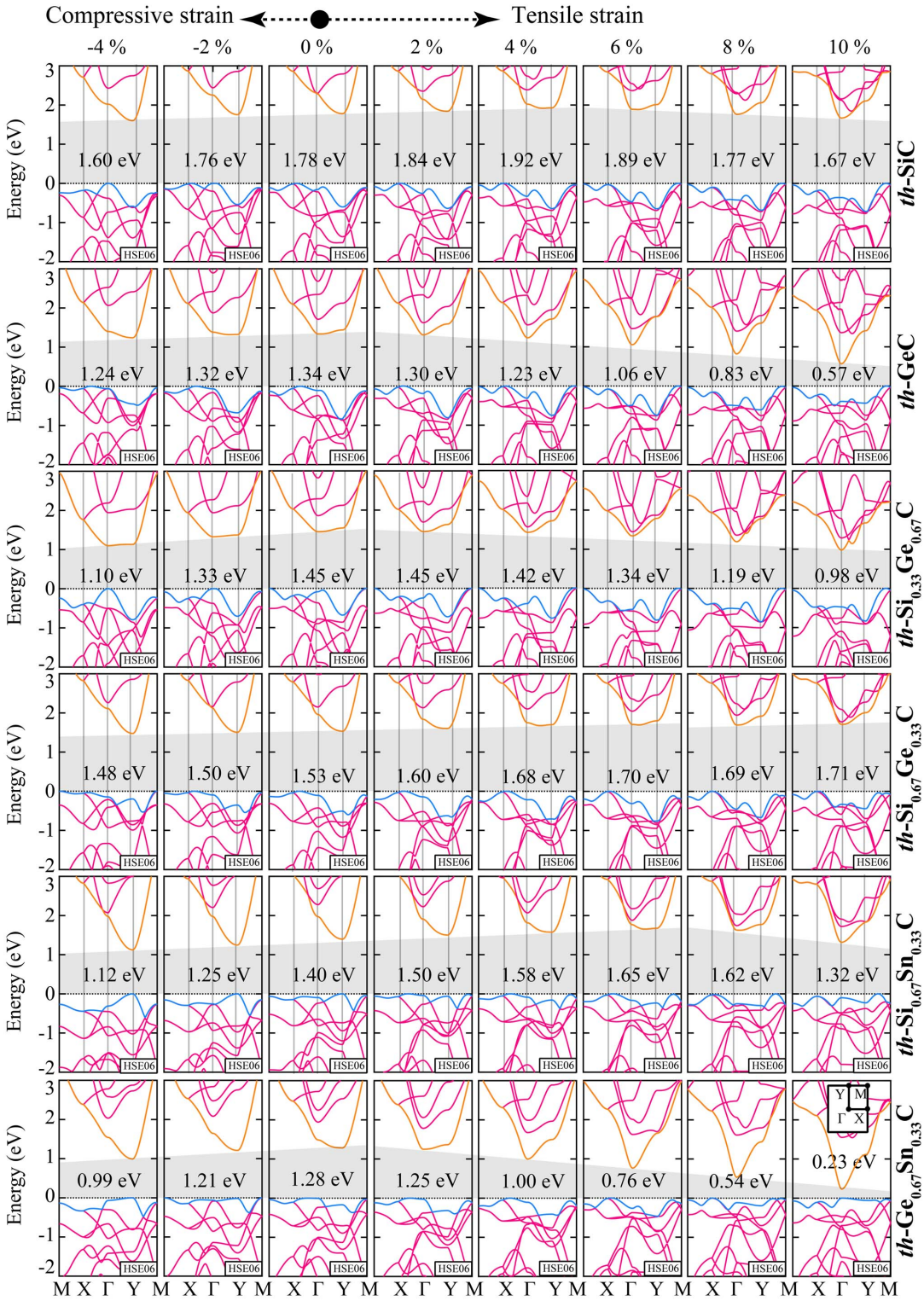

Figure S14: Strain engineering on the electronic band structure of *th*-XC compounds subjected to equi-biaxial compression and tensile strains. Positive and negative strains refer to tension and compression, respectively. The VBM and CBM energies calculated by the HSE06 functional method for each strain are depicted in blue and pink, respectively. The strain- induced band gap energy value is given for each strain point, and its variation are depicted by shaded region.

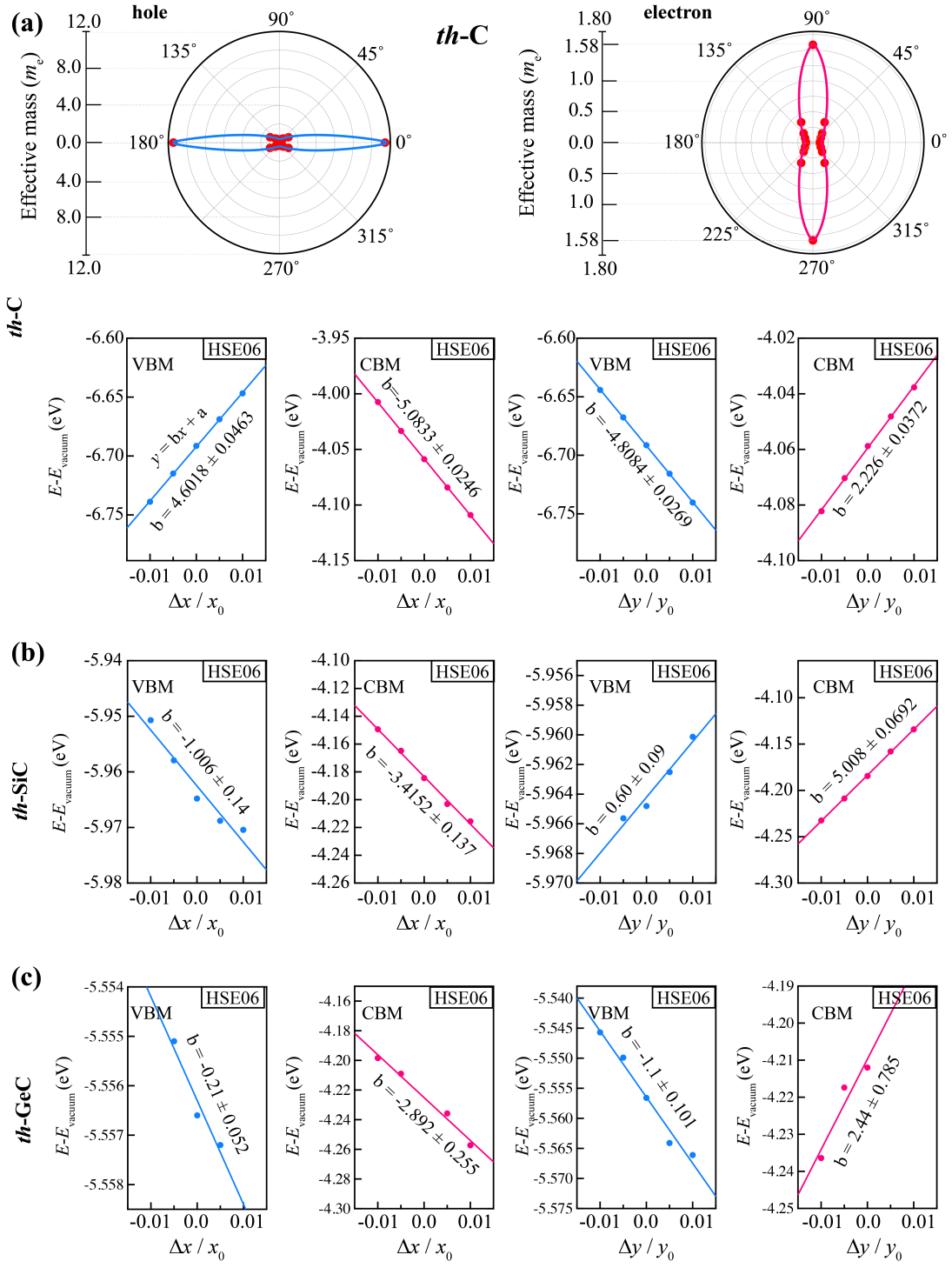

Figure S15: (a) Angular dispersion of electron and hole effective mass (calculated by the HSE06 functional) of *th*-C upper panel, dependence of total energy (calculated by the HSE06 functional) of band edges (CBM and VBM positions) *versus* the vacuum level as a function of applied uniaxial strains along the transport direction for *th*-C lower panel, (b) *th*-SiC, and (c) *th*-GeC.

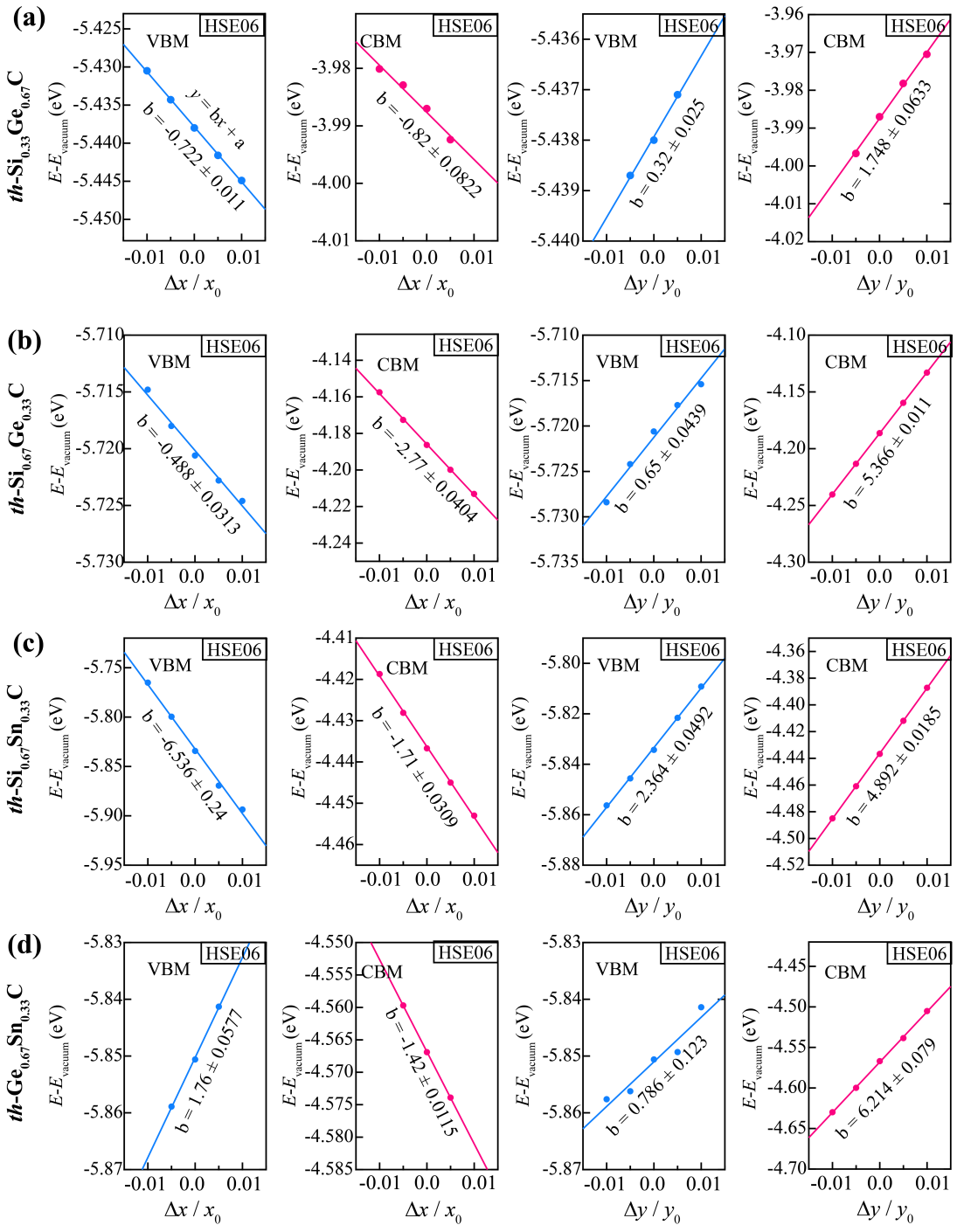

Figure S16: Dependence of total energy (calculated by the HSE06 functional) of band edges (CBM and VBM positions) *versus* the vacuum level as a function of applied uniaxial strains along the transport direction for (a) *th*-$Si_{0.33}Ge_{0.67}C$, (b) *th*-$Si_{0.67}Ge_{0.33}C$, (c) *th*-$Si_{0.67}Sn_{0.33}C$, and (d) *th*-$Ge_{0.67}Sn_{0.33}C$.